



Cite this: *RSC Adv.*, 2020, 10, 37743

# One-pot synthesis of poly(ionic liquid)s with 1,2,3-triazolium-based backbones *via* clickable ionic liquid monomers†

Ruka Hirai, Tatsuki Hibino, Takaichi Watanabe, Takashi Teranishi  
and Tsutomu Ono \*

Clickable  $\alpha$ -azide- $\omega$ -alkyne ionic liquid monomers were developed and subsequently applied to the one-pot synthesis of ionically conducting poly(ionic liquid)s with 1,2,3-triazolium-based backbones through a click chemistry strategy. This approach does not require the use of solvents, polymerisation mediators, or catalysts. The obtained poly(ionic liquid)s were characterized by NMR, differential scanning calorimetry, thermogravimetric analysis, and impedance spectroscopy analysis. Moreover, these poly(ionic liquid)s were cross-linked *via* *N*-alkylation with a dianion quarternizing agent to achieve enhanced ionic conductivity and mechanical strength. The resulting free-standing films showed a Young's modulus up to 4.8 MPa and ionic conductivities up to  $4.60 \times 10^{-8} \text{ S cm}^{-1}$  at 30 °C. This facile synthetic strategy has the potential to expand the availability of poly(ionic liquid)s and promote the development of functional materials.

Received 17th September 2020

Accepted 7th October 2020

DOI: 10.1039/d0ra07948k

rsc.li/rsc-advances

## Introduction

Poly(ionic liquid)s (PILs) are a type of polyelectrolyte in which the repeat unit is an ionic liquid (IL). PILs exhibit the unique physicochemical properties of low-molecular-weight ILs (*e.g.* high ionic conductivity, thermal stability, and chemical stability) as well as polymeric properties (*e.g.* mechanical stability, processability, and macromolecular tunability). So far various kinds of PIL materials including cross-linked PILs, PIL block copolymers, and PIL-based ion gels<sup>1–3</sup> have been developed as IL-based soft materials, since they offer advantages for various applications including dye-sensitised solar cells, fuel cells, electrochromic devices, membranes, sensors and actuators, batteries, and supercapacitors.<sup>4–10</sup> In addition, a broad spectrum of PILs with different combinations of cations (*e.g.* ammonium, pyridinium, imidazolium, phosphonium, and triazolium) and anions (*e.g.* halides, inorganic fluoride, and perfluorinated sulfonimides) have been designed to provide materials with task-specific IL properties.<sup>11,12</sup>

Recently, 1,2,3-triazolium-based PILs (TPILs) have been developed as a structurally rich family of PILs.<sup>13</sup> TPILs are generally synthesised by combining step-growth or chain-growth polymerisation methods with copper-catalysed azide-alkyne cycloaddition click chemistry using diazide and dialkyne

or  $\alpha$ -azide- $\omega$ -alkyne monomers, followed by 1,2,3-triazole *N*-alkylation.<sup>14</sup> The synthesis of TPILs using click chemistry has attracted particular attention because the reaction is efficient and orthogonal, which offers unprecedented opportunities to broaden the functionality of macromolecular design for polymer solid electrolytes. Moreover, Puguang *et al.* recently reported that PILs with backbones based on 1,2,3-triazole (backbone TPILs) with oxyethylene spacers exhibit the highest ionic conductivities ( $10^{-4} \text{ S cm}^{-1}$  at 30 °C) among known backbone PILs.<sup>15</sup> This finding suggests that the design and characterization of a broad library of backbone TPILs is important for realizing innovative functional materials, thus necessitating the development of simple synthetic strategies for backbone TPILs. Over the last few years, various types of TPILs with tailored structures, including ionenes, poly(acrylate)s, poly(vinyl ester)s, poly(styrene)s, and polypeptoids have been developed.<sup>16–20</sup> However, to the best of our knowledge, the synthesis of backbone TPILs using clickable IL monomers has not been reported.

In this study, we synthesised backbone TPILs *via* the polyaddition of clickable  $\alpha$ -azide- $\omega$ -alkyne IL monomers with a 1,2,3-triazolium cation and iodide(I) or bis(trifluoromethanesulfonyl)imide (Tf<sub>2</sub>N) counter anions. Here, polyaddition was achieved using thermal azide-alkyne cycloaddition (TAAC), a type of one-step click chemistry that does not require the use of solvents, polymerisation mediators, or catalysts. Moreover, the 1,2,3-triazole-based backbones of the obtained TPILs could be *N*-alkylated using a difunctionalised quarternizing agent to produce cross-linked TPILs with twice the number of IL moieties in the polymer backbone and a higher mechanical strength than the precursor TPILs. We

Department of Applied Chemistry, Graduate School of Natural Science, Okayama University, 3-1-1, Tsushima-naka, Kita-ku, Okayama, 700-8530, Japan. E-mail: [tono@okayama-u.ac.jp](mailto:tono@okayama-u.ac.jp); Fax: +81-86-251-8083; Tel: +81-86-251-8083

† Electronic supplementary information (ESI) available. See DOI: 10.1039/d0ra07948k



report the above mentioned facile synthetic methodology to obtain TPILs with clickable  $\alpha$ -azide- $\omega$ -alkyne IL monomers through click chemistry and cross-linked TPILs *via* subsequent quarternizing reaction. Then, we investigate the effect of the amount of cross-linking agent on the mechanical strength as well as the ionic conductivity of the resultant cross-linked TPILs.

## Experimental

### Materials

Diisopropylethylamine (DIPEA, 97%), benzyl azide (94%), copper(II) acetate ( $\text{Cu}(\text{OAc})_2$ , 97%), Super-dehydrated acetonitrile (99.8%), *N,N*-dimethylformamide (99.5%), and sodium azide (98%) were purchased from FUJIFILM Wako Pure Chemical Corp. 5-Chloro-1-pentyne (96%), lithium bis(trifluoromethanesulfonyl)imide ( $\text{LiTf}_2\text{N}$ , 98%), and 1,4-diiodobutane (98%) were purchased from Tokyo Chemical Industry Co., Ltd. 6-Iodo-1-hexyne (97%) was purchased from Aldrich. All chemicals were used as received.

### Characterization methods

$^1\text{H}$  NMR (400 MHz),  $^{13}\text{C}$  NMR (100 MHz), and  $^{19}\text{F}$  NMR (376.5 MHz) spectra were recorded on a Varian 400-MR spectrometer in  $\text{DMSO}-d_6$  using solvent peaks (2.5 ppm) as internal references. Gel permeation chromatography (GPC) was carried out at 40 °C using a chromatograph (HLC-8120 GPC, Tosoh Ltd.) connected to a refractive index detector and columns (TSK guard column Super AW-H, TSKgel Super AWM-H, TSKgel Super HM-H, and TSKgel Super H4000). The eluent was 60 mM  $\text{LiTf}_2\text{N}$  in *N,N*-dimethylformamide (DMF) at a flow rate of 0.3 mL  $\text{min}^{-1}$ . The weight-average molecular weight ( $M_w$ ), number-average molecular weight ( $M_n$ ), and molecular weight dispersity ( $M_w/M_n$ ) were calculated from a calibration curve based on polystyrene standards. Differential scanning calorimetry (DSC) measurements were carried out under nitrogen using a DSC 6100 instrument (Seiko Instruments Inc.) at a heating rate of 10 °C  $\text{min}^{-1}$ . Glass transition temperature ( $T_g$ ) values were measured during the second heating cycle. Thermogravimetric analysis (TGA) was performed under nitrogen using a DTG-60 instrument (Shimadzu Co.) at a heating rate of 10 °C  $\text{min}^{-1}$ . Scanning electron microscopy (SEM) and energy dispersive X-ray spectroscopy (EDX) analyses were performed using a JMT-IT100LV instrument (JEOL Ltd.) operated at 15.0 kV. Before observation, the samples were coated with Au. The mechanical properties of cross-linked TPILs **5a–d** were evaluated using an automatic recording universal testing instrument (EZ Test EZ-SX 500 N, Shimadzu Co.) at room temperature. The sample films were cut into dumbbell-shaped specimens with a length, width, and thickness of 35, 2, and 0.4 mm, respectively. The specimens were tested at a cross-head rate of 10 mm  $\text{min}^{-1}$  using an initial gauge length of 15 mm. The swelling behaviour of the cross-linked TPILs was evaluated by measuring the weights of cross-linked TPILs **5a–d** after immersion in  $[\text{Bmim}][\text{Tf}_2\text{N}]$ . At 1, 2, 3, 6, 9, 12, 24, 36, 48, 72, 96, and 110 h after the onset of the experiment, the samples were removed from the

$[\text{Bmim}][\text{Tf}_2\text{N}]$  bath and their weights were recorded. Subsequently, the samples were reimmersed in the same bath. The changes in sample weight were plotted as a function of immersion time, with the initial sample weight defined as 100 wt%. Ionic conductivities were measured using an impedance analyser (Model 4294A, Keysight). Samples were prepared using the following methods. TPIL **3** was pressed using a hot press (IMC-1A45, Imoto Machinery Co., Ltd.), and the thickness was controlled by employing a 114  $\mu\text{m}$  thick polytetrafluoroethylene (PTFE) spacer. TPIL **4** in acetonitrile was cast onto a Cu electrode and annealed at 80 °C under vacuum. Another Cu electrode was then placed on top of the polymer films using a 114  $\mu\text{m}$  thick PTFE spacer to prepare a measurement cell. Cross-linked TPILs **5a–d** were coated (Quick Coater CC701, Sanyu Electron Co., Ltd.) with Au to prepare measurement cells. Frequency sweeps were then performed isothermally at  $10^7$  to 40 Hz by applying a sinusoidal potential of 1 V over a temperature range of 130 to 20 °C in steps of 10 °C.

### Synthesis of chlorinated-1,2,3-triazole<sup>21</sup>

DIPEA (2 mmol, 0.345 mL) was added to 65 mL of dry acetonitrile solution containing  $\text{Cu}(\text{OAc})_2$  (1 mmol, 0.182 g), 5-chloro-1-pentyne (20 mmol, 2.12 mL), and benzyl azide (20 mmol, 2.50 mL) under stirring. The reaction mixture was stirred in the dark at room temperature for 24 h, and then the solvent was evaporated. The crude product was purified by column chromatography (hexane/ethyl acetate = 4 : 1) to give chlorinated-1,2,3-triazole as a slightly yellow solid (3.48 g, 14.8 mmol, 74%).  $^1\text{H}$  NMR (400 MHz,  $\text{DMSO}-d_6$ ,  $\delta$ ): 7.96 (s, 1H), 7.40–7.28 (m, 5H), 5.55 (s, 2H), 3.67 (t,  $J$  = 6.5 Hz, 2H), 2.75 (t,  $J$  = 7.5 Hz, 2H), 2.04 (quin,  $J$  = 7.0 Hz, 2H).  $^{13}\text{C}$  NMR (100 MHz,  $\text{DMSO}-d_6$ ,  $\delta$ ): 145.9, 136.1, 128.6, 127.9, 127.8, 122.1, 52.8, 44.5, 31.7, 22.3.

### Synthesis of azido-1,2,3-triazole

A solution of chlorinated-1,2,3-triazole (20 mmol, 4.71 g) and sodium azide (24 mmol, 1.56 g) in DMF (25 mL) was stirred at 50 °C for 24 h. The crude reaction mixture was quenched with saturated  $\text{NH}_4\text{Cl}$  aq. and then extracted with ethyl acetate (3  $\times$  100 mL). The resulting organic layer was washed with water (2  $\times$  100 mL) and saturated brine (2  $\times$  100 mL), and dried with  $\text{MgSO}_4$ . The solvent was then evaporated to give azido-1,2,3-triazole as a yellow liquid (3.98 g, 14.8 mmol, 82%).  $^1\text{H}$  NMR (400 MHz,  $\text{DMSO}-d_6$ ,  $\delta$ ): 7.95 (s, 1H), 7.40–7.25 (m, 5H), 5.55 (s, 2H), 3.38 (t,  $J$  = 6.5 Hz, 2H), 2.68 (t,  $J$  = 7.9 Hz, 2H), 1.85 (quin,  $J$  = 7.2 Hz, 2H).  $^{13}\text{C}$  NMR (100 MHz,  $\text{DMSO}-d_6$ ,  $\delta$ ): 146.2, 136.1, 128.6, 127.9, 127.7, 122.0, 52.8, 50.1, 28.0, 22.1.

### Synthesis of $\alpha$ -azide- $\omega$ -alkyne IL monomer **1**

A solution of azido-1,2,3-triazole (10 mmol, 2.1 mL) and 6-iodo-1-hexyne (15 mmol, 2.0 mL) in dry acetonitrile (20 mL) was stirred in the dark at 50 °C for 120 h. Following solvent evaporation, the crude product was precipitated five times with diethyl ether. After drying under vacuum, **1** was recovered as an orange viscous liquid (2.35 g, 5.22 mmol, 52%).  $^1\text{H}$  NMR (400 MHz,  $\text{DMSO}-d_6$ ,  $\delta$ ): 8.90 (s, 1H), 7.48–7.42 (m, 5H), 5.85 (s, 2H), 4.56 (t,  $J$  = 7.7 Hz, 2H), 3.48 (t,  $J$  = 6.7 Hz, 2H), 2.92 (t,  $J$  = 7.9 Hz,



2H), 2.83 (t,  $J = 2.7$  Hz, 1H), 2.23 (td,  $J = 7.3, 2.8$  Hz, 2H), 2.01–1.90 (m, 4H), 1.50 (quin,  $J = 7.4$  Hz, 2H).  $^{13}\text{C}$  NMR (100 MHz,  $\text{DMSO}-d_6$ ,  $\delta$ ): 143.2, 132.7, 129.1, 128.9, 128.8, 128.6, 83.5, 71.4, 56.1, 50.7, 49.3, 27.1, 26.1, 24.5, 20.4, 17.3. Elemental analysis (%): calculated C, 48.0; H, 5.2; N, 18.7; found C, 46.8; H, 5.2; N, 17.6.

### Synthesis of $\alpha$ -azide- $\omega$ -alkyne IL monomer 2

A solution of **1** (8.50 mmol, 3.83 g) and  $\text{LiTf}_2\text{N}$  (9.35 mmol, 2.68 g) in water (25 mL) was stirred in the dark at 40 °C for 24 h. The reaction mixture was precipitated five times in water to yield after drying under vacuum **2** as a slightly yellow viscous liquid (4.36 g, 7.22 mmol, 85%).  $^1\text{H}$  NMR (400 MHz,  $\text{DMSO}-d_6$ ,  $\delta$ ): 8.90 (s, 1H), 7.45–7.41 (m, 5H), 5.85 (s, 2H), 4.56 (t,  $J = 7.5$  Hz, 2H), 3.48 (t,  $J = 6.9$  Hz, 2H), 2.92 (t,  $J = 7.7$  Hz, 2H), 2.83 (t,  $J = 2.7$  Hz, 1H), 2.23 (td,  $J = 7.2, 2.8$  Hz, 2H), 2.01–1.90 (m, 4H), 1.50 (quin,  $J = 7.3$  Hz, 2H).  $^{13}\text{C}$  NMR (100 MHz,  $\text{DMSO}-d_6$ ,  $\delta$ ): 143.4, 132.5, 129.1, 128.9, 128.7, 128.4, 119.5 (q,  $J = 320$  Hz, 2C), 83.4, 70.8, 56.3, 50.0, 49.5, 26.9, 25.8, 24.3, 19.9, 17.0. Elemental analysis (%): calculated C, 39.8; H, 3.8; N, 16.2; found C, 39.5; H, 3.8; N, 16.2.  $^{19}\text{F}$  NMR (376.5 MHz,  $\text{DMSO}-d_6$ ,  $\delta$ ): –78.5 (6F).

### Synthesis of TPIL 3

IL monomer **1** (100 mg, 0.22 mmol) was stirred at 110 °C for 24 h. The resulting polymer was precipitated in acetone and then dried under vacuum to yield **3** as a dark brown material (90 mg, 90%).  $^1\text{H}$  NMR (400 MHz,  $\text{DMSO}-d_6$ ,  $\delta$ ): 8.89 (bs, 1H), 7.88 (s, 1H), 7.48–7.39 (m, 5H), 5.84 (bs, 2H), 4.73–4.20 (m, 4H), 3.06–2.85 (m, 2H), 2.79–2.58 (m, 2H), 2.39–2.10 (m, 2H), 2.04–1.87 (m, 2H), 1.74–1.53 (m, 2H).

### Synthesis of TPIL 4

IL monomer **2** (100 mg, 0.17 mmol) was stirred at 110 °C for 24 h. The resulting polymer was precipitated in ethyl acetate and then dried under vacuum to yield **4** as a brown sticky material (92 mg, 92%).  $^1\text{H}$  NMR (400 MHz,  $\text{DMSO}-d_6$ ,  $\delta$ ): 8.89 (bs, 1H), 7.88 (s, 1H), 7.48–7.39 (m, 5H), 5.85 (bs, 2H), 4.74–4.24 (m, 4H), 3.07–2.85 (m, 2H), 2.78–2.57 (m, 2H), 2.41–2.10 (m, 2H), 2.07–1.86 (m, 2H), 1.74–1.51 (m, 2H).  $^{19}\text{F}$  NMR (376.5 MHz,  $\text{DMSO}-d_6$ ,  $\delta$ ): –78.5 (6F).

### Synthesis of cross-linked TPILs 5a–d

1,4-Diiodobutane (0.5, 1.0, 1.5, or 2.0 equiv.) was added to a solution of TPIL **3** (800 mg, 1.78 mmol triazole groups, 1.0 equiv.) in DMF (3.0 mL). The mixture was stirred at room temperature for 30 min. Subsequently, the reaction mixture was injected into a mould consisting of two glass plates with a fluorinated ethylene propylene film and a PTFE spacer with a thickness of 1 mm. Heating at 110 °C in an oven for 12 h yielded a brown film. The iodide-containing film was added to a 5 wt%  $\text{LiTf}_2\text{N}$  solution in acetonitrile/water (3 : 1) at 50 °C for 48 h. The resulting film was washed with acetonitrile/water (3 : 1) and dried at 100 °C under vacuum.

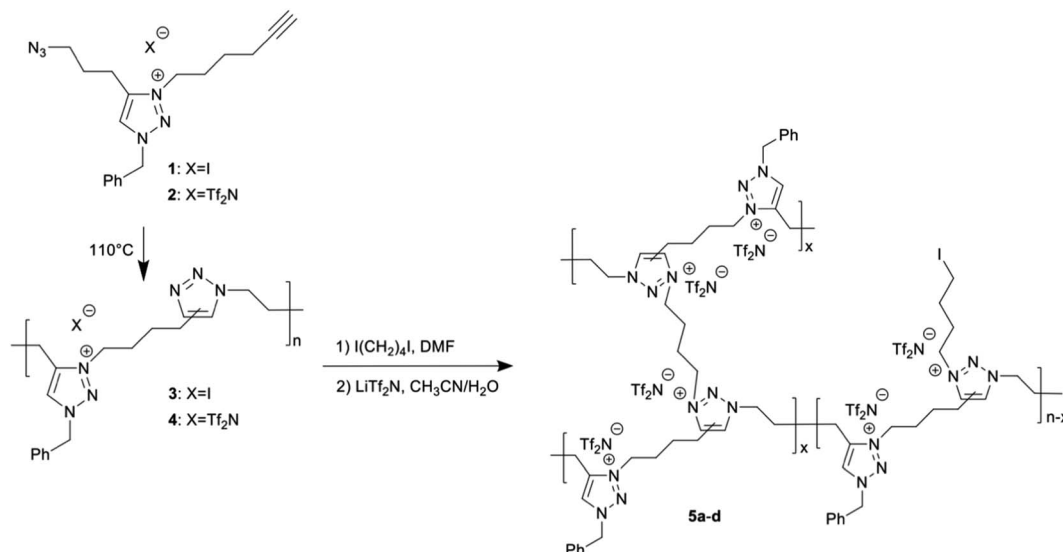
## Results and discussion

$\alpha$ -Azide- $\omega$ -alkyne IL monomers **1** and **2** were prepared in three or four steps (Scheme S1†). The successful synthesis of each compound was confirmed by  $^1\text{H}$  and  $^{13}\text{C}$  NMR spectroscopy (Fig. S1–S4†), and the purities of the IL monomers were evaluated by elemental analysis.  $^1\text{H}$  NMR spectrum of IL monomer **1** (Fig. S3†) clearly showed the synthesis of  $\alpha$ -azide- $\omega$ -alkyne IL monomer with a 1,2,3-triazolium cation. Indeed, besides the disappearance of the signal at 8.0 ppm attributed to the 1,2,3-triazole moiety, new signals were confirmed at 8.9 ppm for the 1,2,3-triazolium proton and at 2.8 and 3.5 ppm for propargyl and azidomethylene chain ends, respectively. TPILs **3** and **4** were obtained by polymerisation of IL monomers **1** and **2** at 110 °C for 24 h *via* TAAC (Scheme 1) as a dark brown material and brown sticky material, respectively. The successful synthesis of both samples was confirmed by  $^1\text{H}$  NMR spectroscopy (Fig. S5 and S6†). All of the  $^1\text{H}$  NMR peaks were broad due to shorter relaxation time of the high-molecular-weight polymer. In both cases,  $^1\text{H}$  NMR confirmed the polymerisation of IL monomers by the appearance of the proton signals of the 1,2,3-triazole ring at 7.9 ppm as well as the absence of signals corresponding to propargyl and azidomethylene chain ends. Only TPIL **4** could be characterised by gel permeation chromatography (GPC) using a 60 mM solution of  $\text{LiTf}_2\text{N}$  in *N,N*-dimethylformamide (DMF) as ref. 22 This analysis revealed a number-average molar mass of 28 000 g mol $^{-1}$  with a molecular weight dispersity of 3.3 for TPIL **4** (Fig. S7†).

The solubilities of IL monomers **1** and **2** and TPILs **3** and **4** were investigated in water and common organic solvents (Table S1†). IL monomer **1** was water-soluble but IL monomer **2** was water-insoluble. This trend is in agreement that halide is hydrophilic anion and  $\text{Tf}_2\text{N}$  is hydrophobic anion.<sup>23</sup> Both the IL monomers were soluble in all the examined organic solvents, except for diethyl ether ( $\text{Et}_2\text{O}$ ). TPILs **3** and **4** were insoluble in methanol (MeOH) and dichloromethane ( $\text{CH}_2\text{Cl}_2$ ), but only TPIL **4** was soluble in acetone and  $\text{CH}_3\text{CN}$ . This solubility of TPIL **4** allows easy processing as membranes and coating using solvents that can be easily eliminated by evaporation or solvent extraction.

Cross-linked PILs **5a–d** were prepared in two steps (Scheme 1). First, a mixture of TPIL **3**, 1,4-diiodobutane as a cross-linking agent, and DMF was injected into a mould and heated at 110 °C for 12 h to yield cross-linked TPILs with I anions. The amount of cross-linking agent was varied from 0.5 to 2.0 equiv. relative to the triazole groups in TPIL **3**. Then, the cross-linked TPILs with I anions were added to a mixture of  $\text{LiTf}_2\text{N}$  and acetonitrile/water (3 : 1) at 50 °C for 48 h to yield **5a–d** as slightly yellow films (Fig. 1). In comparison with TPIL **4**, these films were free-standing and unchanged shape at high temperature. A conversion of 87.9 mol% for the anion exchange process was confirmed by scanning electron microscopy-energy-dispersive X-ray spectroscopy (SEM-EDX) (Fig. S8†).

The thermal properties of TPILs **3** and **4** and cross-linked TPILs **5a–d** were characterised by differential scanning calorimetry (DSC) and thermogravimetric analysis (TGA) (Table 1).



Scheme 1 Synthesis of TPILs **3** and **4** and cross-linked TPILs **5a–d** using clickable IL monomers.

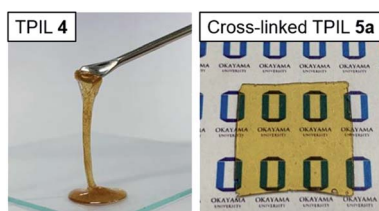


Fig. 1 Photographs of TPIL **4** (left) and cross-linked TPIL **5a** (right).

TPIL **4** with  $\text{Tf}_2\text{N}$  anions showed a lower glass transition temperature value ( $T_g = 7.4^\circ\text{C}$ ) than TPIL **3** with  $\text{I}$  anions ( $T_g = 38.3^\circ\text{C}$ ). This difference can be explained by the sizes of the anions, as the larger  $\text{Tf}_2\text{N}$  anion has a greater ability to hinder interactions between polymer chains, thus decreasing both the chain packing density and  $T_g$ .<sup>24</sup> Cross-linked TPILs **5a–d** showed higher  $T_g$  values ( $19.0$ – $22.0^\circ\text{C}$ ) than TPIL **4** with  $\text{Tf}_2\text{N}$  anions owing to immobilisation of the polymer chains. However, the amount of cross-linking agent did not significantly affect  $T_g$ . This is probably because  $T_g$  would depend on the mobility of polymer chains forming a cross-linked network. The TGA curves showed that TPIL **3** with  $\text{I}$  anions started to degrade near  $200^\circ\text{C}$ ,

whereas TPIL **4** and cross-linked TPILs **5a–d** with  $\text{Tf}_2\text{N}$  anions started to degrade near  $300^\circ\text{C}$  (Fig. 2). This behaviour is attributed to the difference in the nucleophilicities of these anions.

The mechanical properties of cross-linked TPILs **5a–d** were evaluated by tensile tests under ambient conditions, and representative stress–strain curves are shown in Fig. 3. TPIL **4** was a sticky material but cross-linked TPILs **5a–d** were free-standing films with a Young's modulus in the range of  $0.8$ –

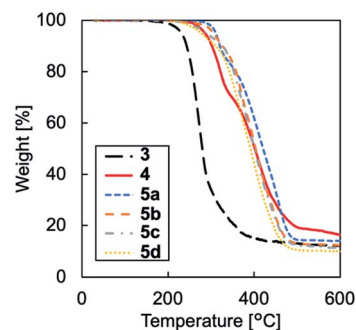


Fig. 2 TGA curves of TPILs **3**, **4** and cross-linked TPILs **5a–d**.

Table 1 Physical properties of TPILs **3**, **4** and cross-linked TPILs **5a–d**

Polymer	Ratio <sup>a</sup>	$T_g^b$ [ $^\circ\text{C}$ ]	$T_{d10}^c$ [ $^\circ\text{C}$ ]	Young's modulus <sup>d</sup> [MPa]	$\sigma_{DC}$ at $30^\circ\text{C}^e$ [ $\text{S cm}^{-1}$ ]	$\sigma_{\infty}^f$ [ $\text{S cm}^{-1}$ ]	$B^f$ [K]	$T_0^f$ [K]
<b>3</b>	0	38.3	243	—	—	0.71	1468	277
<b>4</b>	0	7.4	302	—	$1.16 \times 10^{-8}$	0.41	1089	241
<b>5a</b>	0.5	22.0	320	$0.90 \pm 0.025$	$1.66 \times 10^{-9}$	0.020	978	241
<b>5b</b>	1.0	19.0	327	$4.79 \pm 0.45$	$1.89 \times 10^{-9}$	0.019	987	240
<b>5c</b>	1.5	20.5	327	$2.34 \pm 0.27$	$8.49 \times 10^{-9}$	0.019	968	237
<b>5d</b>	2.0	21.4	311	$0.77 \pm 0.09$	$4.60 \times 10^{-8}$	0.025	858	241

<sup>a</sup> Molar ratio of diiodide to triazole groups. <sup>b</sup> Obtained by DSC. <sup>c</sup> Obtained by TGA. <sup>d</sup> Obtained from tensile tests. <sup>e</sup> Obtained using an impedance analyser. <sup>f</sup> Obtained from VFT fits of the experimental data using eqn (1).





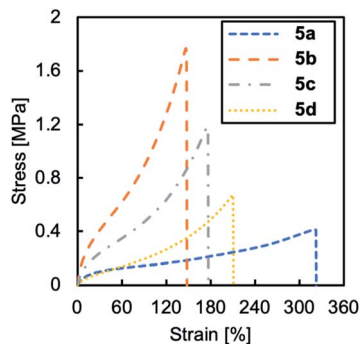


Fig. 3 Stress-strain curves of cross-linked TPILs 5a–d.

4.8 MPa. As the amount of cross-linking agent (molar ratio of diiodide to triazole groups) increased from 0 to 1.0, the Young's modulus of the cross-linked TPILs significantly increased and reached the highest value (4.79 MPa) at the molar ratio of 1.0. This is because a polymer network with a higher cross-link density are formed as increasing the amount of cross-linking agent in this region. On the other hand, as the amount of cross-linking agent (the molar ratio) increased from 1.0 to 2.0, the Young's modulus of the cross-linked TPILs decreased. In the case of **5c** and **5d**, the molar amounts of iodide in the cross-linking agent are much higher than the amount of 1,2,3-triazole groups in TPILs. Hence, it is likely that only one end of most of the cross-linking agents reacts with a triazole groups, causing dangling chains and leading to a polymer network with a lower cross-link density.<sup>25</sup> Based on this assumption, the cross-link densities of the cross-linked TPILs can be summarised as follows: **5a** < **5d** < **5c** < **5b**. This order is consistent with the cross-link density trend estimated from the swelling behaviour of the cross-linked TPILs. In particular, faster swelling speeds were shown as the cross-link density of the material decreased (Fig. 4).

The temperature dependence of the DC conductivity ( $\sigma_{DC}$ ) of TPILs **3** and **4** and cross-linked TPILs **5a–d** were evaluated by impedance spectroscopy analysis over the range of 40 to  $10^7$  Hz. The data were collected at temperatures from 20 to 130 °C with steps of 10 °C. The  $\sigma_{DC}$  values of above mentioned specimens were plotted as a function of inverse temperature (Fig. 5). As generally observed for polymeric materials, the temperature

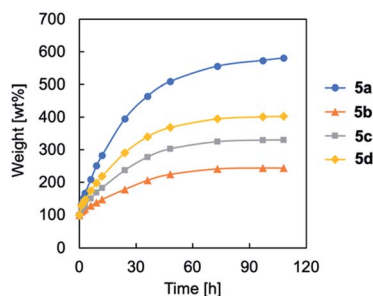


Fig. 4 Swelling behaviour of cross-linked TPILs 5a–d prepared with different amount of cross-linking agent as a function of immersion time.

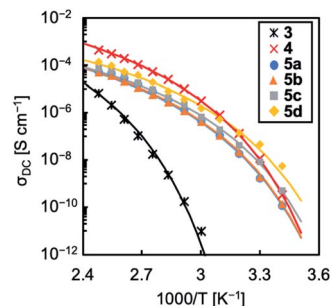


Fig. 5 Direct current conductivity versus inverse temperature for TPILs **3** and **4** and cross-linked TPILs **5a–d**. The solid lines are the VFT fits of the experimental data obtained using the  $\sigma_{\infty}$ ,  $B$ , and  $T_0$  parameters listed in Table 1.

evolution of the  $\sigma_{DC}$  above  $T_g$  follows the Vogel–Fulcher–Tammann (VFT) relation describing the correlation between the charge transport capability of the ionic moieties and the molecular mobility of the polymer chains. Thus, the experimental data were fitted to the VFT equation:

$$\sigma_{DC} = \sigma_{\infty} \exp\left(\frac{-B}{T - T_0}\right) \quad (1)$$

where  $\sigma_{\infty}$  is the ionic conductivity in the limit of high temperature,  $B$  is a fitting parameter related to the activation energy of ionic conduction, and  $T_0$  is the Vogel temperature. The fitted values are summarised in Table 1.

The ionic conductivity of TPIL **4** with  $\text{TF}_2\text{N}$  anions was higher than that of TPIL **3** with  $\text{I}^-$  anions. This difference is mainly caused by a lower  $T_g$  value of the TPIL **4** than TPIL **3**, in addition to another possible reason related to the lower dissociation energy of the ion pairs in TPIL **4** owing to the delocalisation of the  $\text{TF}_2\text{N}^-$  anion. The  $\sigma_{DC}$  values increased from  $1.7 \times 10^{-9}$  to  $4.6 \times 10^{-8} \text{ S cm}^{-1}$ , with the order: **5a** < **5b** < **5c** < **5d**. As the  $T_g$  values of these four samples were comparable, higher  $\sigma_{DC}$  with increasing of molar ratio of diiodide could originate from the higher concentration of mobile  $\text{TF}_2\text{N}^-$  anions as well as the enhanced mobility of  $\text{TF}_2\text{N}^-$  anions by increasing of the dangling chains number. Similarly, the  $\sigma_{DC}$  value of cross-linked TPIL **5d** at 30 °C was higher than that of TPIL **4**.

## Conclusions

We developed new clickable  $\alpha$ -azide- $\omega$ -alkyne IL monomers and a simple method to synthesise backbone TPILs *via* TAAC of these monomers. This synthesis method allows the preparation of TPILs in the absence of solvents, polymerisation mediators, or catalysts, and the resultant TPILs showed ionic conductivity. As the TPILs possessed 1,2,3-triazole-based backbones, *N*-alkylation using a difunctionalised quarternizing agent resulted in cross-linked TPILs that theoretically could contain twice the number of IL moieties in their polymer backbones compared with the precursor TPILs. Further, the Young's modulus of the cross-linked TPILs was tuned by changing the molar amount of the cross-linking agent. We believe that our strategy for synthesising backbone TPILs offers opportunities to broaden the



PIL family and develop innovative functional materials applicable to carbon dioxide separation membranes, fuel cells, electrochromic devices, sensors, and actuators.

## Conflicts of interest

There are no conflicts to declare.

## Acknowledgements

Financial support for this work was provided by the JSPS Grants-in-Aid for Scientific Research (KAKENHI) (Grant No. JP18H03854 and JP19K15340). We also acknowledge Prof. T. Uchida for the EDX measurements.

## Notes and references

- 1 M. M. Obadia, B. P. Mudraboyina, A. serghei, D. Montarnal and E. Drockenmuller, *J. Am. Chem. Soc.*, 2015, **137**, 6078.
- 2 Y. Ye, S. Sharick, E. M. Davis, K. I. Winey and Y. A. Elabd, *ACS Macro Lett.*, 2013, **2**, 575.
- 3 T. Watanabe, R. Takahashi and T. Ono, *Soft Matter*, 2020, **16**, 1572.
- 4 G. Wang, L. Wang, S. Zhuo, S. Fang and Y. Lin, *Chem. Commun.*, 2011, **47**, 2700.
- 5 B. Qiu, B. Lin, Z. Si, L. Qiu, F. Chu, J. Zhao and F. Yan, *J. Power Sources*, 2012, **217**, 329.
- 6 R. Marcilla, F. Alcaide, H. Sardon, J. A. Pomposo, C. Pozo-Gonzalo and D. Mecerreyes, *Electrochem. Commun.*, 2006, **8**, 482.
- 7 S. Zulfiqar, M. I. Sarwar and D. Mecerreyes, *Polym. Chem.*, 2015, **6**, 6435.
- 8 E. Margareta, G. B. Fahs, D. L. Inglefield Jr, C. Jangu, D. Wang, J. R. Heflin, R. B. Moore and T. E. Long, *ACS Appl. Mater. Interfaces*, 2016, **8**, 1280.
- 9 K. Yin, Z. Zhang, L. Yang and S.-I. Hirano, *J. Power Sources*, 2014, **258**, 150.
- 10 G. A. Tiruye, D. Muñoz-Torrero, J. Palma, M. Anderson and R. Marcilla, *J. Power Sources*, 2015, **279**, 472.
- 11 A. S. Shaplov, D. O. Ponkratov and Y. S. Vygodskii, *Polym. Sci.*, 2016, **58**(2), 63.
- 12 H. Ohno, *Macromol. Symp.*, 2007, **249–250**, 551.
- 13 M. M. Obadia and E. Drockenmuller, *Chem. Commun.*, 2016, **52**, 2433.
- 14 M. M. Obadia, B. P. Mudraboyina, I. Allaoua, A. Haddane, D. Montarnal, A. Serghei and E. Drockenmuller, *Macromol. Rapid Commun.*, 2014, **35**, 794.
- 15 J. M. C. Puguán, A. R. Jadhav, L. B. Botton and H. Kim, *Sol. Energy Mater. Sol. Cells*, 2018, **179**, 409.
- 16 J. Wu, J. Chen, J. Wang, X. Liao, M. Xie and R. Sun, *Polym. Chem.*, 2016, **7**, 633.
- 17 R. Sood, B. Zhang, A. Serghei, J. Bernard and E. Drockenmuller, *Polym. Chem.*, 2015, **6**, 3521.
- 18 M. M. Obadia, G. Colliat-Dangus, A. Debuigne, A. Serghei, C. Detrembleur and E. Drockenmuller, *Chem. Commun.*, 2015, **51**, 3332.
- 19 M. M. Obadia, B. P. Mudraboyina, A. Serghei, T. N. T. Phan, D. Gígmes and E. Drockenmuller, *ACS Macro Lett.*, 2014, **3**, 658.
- 20 C. Secker, J. W. Robinson and H. Schlaad, *Eur. Polym. J.*, 2015, **62**, 394.
- 21 M. T. Berry, D. Castrejon and E. Hein, *Org. Lett.*, 2014, **16**, 3676.
- 22 H. He, M. Zhong, B. Adzime, D. Luebke, H. Nulwala and K. Matyjaszewski, *J. Am. Chem. Soc.*, 2013, **135**, 4227.
- 23 J. Yuan and M. Antonietti, *Polymer*, 2011, **52**, 1469.
- 24 Y. Ye and Y. A. Elabd, *Polymer*, 2011, **52**, 1309.
- 25 X. Zhou, M. M. Obadia, S. R. Venna, E. A. Roth, A. Serghei, D. R. Luebke, C. Myers, Z. Chang, R. Enick, E. Drockenmuller and H. B. Nulwala, *Eur. Polym. J.*, 2016, **84**, 65.

